First Light Measurements of Capella with the Low Energy Transmission Grating Spectrometer aboard the Chandra X-ray Observatory

A.C. Brinkman, C.J.T. Gunsing, J.S. Kaastra, R.L.J. van der Meer, R. Mewe, F. Paerels [1],
A.J.J. Raassen [2], J.J. van Rooijen

*Space Research Organization of the Netherlands (SRON), Sorbonnelaan 2, 3584 CA   Utrecht,
The Netherlands*

H. Bräuninger, W. Burkert, V. Burwitz, G. Hartner, P. Predehl

*Max-Planck-Institut für Extraterrestrische Physik (MPE), Postfach 1603, D-85740 Garching,
Germany*

J.-U. Ness, J.H.M.M. Schmitt

Universität Hamburg, Gojenbergsweg 122, D-21029 Hamburg, Germany

J.J. Drake, O. Johnson, M. Juda, V. Kashyap, S.S. Murray, D. Pease, P. Ratzlaff, B.J. Wargelin

Harvard-Smithsonian Center for Astrophysics, 60 Garden Street, Cambridge, MA 02138, USA

ABSTRACT

We present the first X-ray spectrum obtained by the Low Energy Transmission Grating Spectrometer (LETGS) aboard the Chandra X-ray Observatory. The spectrum is of Capella and covers a wavelength range of 5–175 Å (2.5–0.07 keV). The measured wavelength resolution, which is in good agreement with ground calibration, is $\Delta\lambda \simeq 0.06$ Å (FWHM). Although in-flight calibration of the LETGS is in progress, the high spectral resolution and unique wavelength coverage of the LETGS are well demonstrated by the results from Capella, a coronal source rich in spectral emission lines. While the primary purpose of this letter is to demonstrate the spectroscopic potential of the LETGS, we also briefly present some preliminary astrophysical results. We discuss plasma parameters derived from line ratios in narrow spectral bands, such as the electron density diagnostics of the He-like triplets of carbon, nitrogen, and oxygen, as well as resonance scattering of the strong Fe XVII line at 15.014 Å.

Subject headings: instrumentation: spectrographs — line: identification — plasmas — stars: individual (Capella) — stars: coronae — X-rays: stars

---

[1]Present address, Columbia University, New York, NY, USA

[2]Also at Astronomical Institute "Anton Pannekoek", Kruislaan 403, 1098 SJ Amsterdam, The Netherlands

1. Introduction

The LETGS consists of three components of the Chandra Observatory: the High Resolution Mirror Assembly (HRMA) (Van Speybroeck et al. 1997), the Low Energy Transmission Grating (LETG) (Brinkman et al. 1987, 1997; Predehl et al. 1997), and the spectroscopic array of the High Resolution Camera (HRC-S) (Murray et al. 1997). The LETG, designed and manufactured in a collaborative effort of SRON in the Netherlands and MPE in Germany, consists of a toroidally shaped structure which supports 180 grating modules. Each module holds three 1.5-cm diameter grating facets which have a line density of 1008 lines/mm. The three flat detector elements of the HRC-S, each 10 cm long and 2 cm wide, are tilted to approximate the Rowland focal surface at all wavelengths, assuring a nearly coma-free spectral image. The detector can be moved in the cross-dispersion direction and along the optical axis, to optimize the focus for spectroscopy. [3]

An image of the LETG spectrum is focused on the HRC-S with zeroth order at the focus position and dispersed positive and negative orders symmetric on either side of it. The dispersion is 1.15 Å/mm in first spectral order. The spectral width in the cross-dispersion direction is minimal at zeroth order and increases at larger wavelengths due to the intrinsic astigmatism of the Rowland circle spectrograph. The extraction of the spectrum from the image is done by applying a spatial filter around the spectral image and constructing a histogram of counts vs. position along the dispersion direction. The background is estimated from areas on the detector away from the spectral image and can be reduced by filtering events by pulse-height.

2. First Light Spectrum

Capella is a binary system at a distance of 12.9 pc consisting of G8 and G1 giants with an orbital period of 104 days (Hummel et al. 1994). It is the brightest quiescent coronal X-ray source in the sky after the Sun, and is therefore an obvious line source candidate for first light and for instrument calibration. X rays from Capella were discovered in 1975 (Catura, Acton, & Johnson 1975; Mewe et al. 1975) and subsequent satellite observations provided evidence for a multi-temperature component plasma (e.g. Mewe (1991) for references). Recent spectra were obtained with EUVE longward of 70 Å with a resolution of about 0.5 Å (Dupree et al. 1993; Schrijver et al. 1995).

The LETG First Light observation of Capella was performed on 6 September 1999 (00h27m UT – 10h04m UT) with LETG and HRC-S. For the analysis we use a composite of six observations obtained in the week after first light, with a total observing time of 95 ksec. The HRC-S output was processed through standard pipeline processing. For LETG/HRC-S events, only the product

---

[3]Further information on LETGS components is found in the AXAF Observatory Guide (http://asc.harvard.edu/udocs/) and at the Chandra X-ray Center calibration webpages (http://asc.harvard.edu/cal/).

of the wavelength and diffraction order is known because no diffraction order information can be extracted. Preliminary analysis of the pipeline output immediately revealed a beautiful line-rich spectrum. The complete background-subtracted, negative-order spectrum between 5 and 175 Å is shown in Fig. 1. Line identifications were made using previously measured and/or theoretical wavelengths from the literature. The most prominent lines are listed in Table 1.

The spectral resolution $\Delta\lambda$ of the LETGS is nearly constant when expressed in wavelength units, and therefore the resolving power $\lambda/\Delta\lambda$ is greatest at long wavelengths. With the current uncertainty of the LETGS wavelength scale of about 0.015 Å, this means that the prominent lines at 150 and 171 Å could be used to measure Doppler shifts as small as 30 km/sec, such as may occur during stellar-flare mass ejections, once the absolute wavelength calibration of the instrument has been established. This requires, however, that line rest-frame wavelengths are accurately known and that effects such as the orbital velocity of the Earth around the Sun are taken into account. Higher-order lines, such as the strong O VIII Lyα line at 18.97 Å, which is seen out to 6th order, can also be used.

3. Diagnostics

A quantitative analysis of the entire spectrum by multi-temperature fitting or differential emission measure modeling yields a detailed thermal structure of the corona, but this requires accurate detector efficiency calibration which has not yet been completed. However, some diagnostics based on intensity ratios of lines lying closely together can already be applied. In this letter we consider the helium-like line diagnostic and briefly discuss the resonance scattering in the Fe XVII 15.014 Å line.

3.1. Electron Density & Temperature Diagnostics

Electron densities, n_e, can be measured using density-sensitive spectral lines originating from metastable levels, such as the forbidden (f) $2^3S \rightarrow 1^1S$ line in helium-like ions. This line and the associated resonance (r) $2^1P \rightarrow 1^1S$ and intercombination (i) $2^3P \rightarrow 1^1S$ line make up the so-called helium-like "triplet" lines (Gabriel & Jordan 1969; Pradhan 1982; Mewe, Gronenschild, & Van den Oord 1985). The intensity ratio $(i+f)/r$ varies with electron temperature, T, but more importantly, the ratio i/f varies with n_e due to the collisional coupling between the 2^3S and 2^3P level.

The LETGS wavelength band contains the He-like triplets from C, N, O, Ne, Mg, and Si ($\sim$ 40, 29, 22, 13.5, 9.2, and 6.6 Å, respectively). However, the Si and Mg triplets are not sufficiently resolved and the Ne IX triplet is too heavily blended with iron and nickel lines for unambiguous density analysis. The O VII lines are clean (see Fig. 2) and the C V and N VI lines can be separated from the blends by simultaneous fitting of all lines. These triplets are suited to diagnose plasmas

in the range $n_e = 10^8$–10^{11} cm^{-3} and $T \sim 1$–3 MK. For the C, N, and O triplets the measured i/f ratios are 0.38 ± 0.14, 0.52 ± 0.15, and 0.250 ± 0.035, respectively, which imply (Pradhan 1982) n_e (in 10^9 cm^{-3}) $= 2.8 \pm 1.3$, 6 ± 3, and $\lesssim 5$ (1σ upper limit), respectively, for typical temperatures as indicated by the $(i+f)/r$ ratios of 1, 1, and 3 MK, respectively. This concerns the lower temperature part of a multi-temperature structure which also contains a hot ($\sim$6–8 MK), and dense ($\gtrsim 10^{12}$ cm^{-3}) compact plasma component (see Section 3.2). The derived densities are comparable to those of active regions on the Sun with a temperature of a few MK. Fig. 2 shows a fit to the O VII triplet measured in the –1 order. The He-like triplet diagnostic, which was first applied to the Sun (e.g., Acton et al. (1972); Wolfson, Doyle, & Phillips (1983)) has now for the first time been applied to a star other than the Sun.

The long-wavelength region of the LETGS between 90 and 150 Å contains a number of density-sensitive lines from 2ℓ–$2\ell'$ transitions in the Fe-L ions Fe XX–XXII which provide density diagnostics for relatively hot ($\gtrsim 5$ MK) and dense ($\gtrsim 10^{12}$ cm^{-3}) plasmas (Mewe, Gronenschild, & Van den Oord 1985; Mewe, Lemen, & Schrijver 1991; Brickhouse, Raymond & Smith 1995). These have been applied in a few cases to EUVE spectra of late-type stars and in the case of Capella have suggested densities more than two orders of magnitude higher than found here for cooler plasma (Dupree et al. 1993; Schrijver et al. 1995). These diagnostics will also be applied to the LETGS spectrum as soon as the long-wavelength efficiency calibration is established.

3.2.   The 15–17 Å region: resonance scattering of Fe XVII?

Transitions in Ne-like Fe XVII yield the strongest emission lines in the range 15–17 Å (cf. Fig. 1). In principle, the optical depth, τ, in the 15.014 Å line can be obtained by applying a simplified escape-factor model to the ratio of the Fe XVII 15.014 Å resonance line with a large oscillator strength to a presumably optically thin Fe XVII line with a small oscillator strength. We use the 15.265 Å line because the 16.780 Å line can be affected by radiative cascades (Liedahl 1999). Solar physicists have used this technique to derive the density in active regions on the Sun (e.g., Saba et al. (1999); Phillips et al. (1996, 1997)).

Various theoretical models predict 15.014/15.265 ratio values in the range 3.3–4.7 with only a slow variation ($\lesssim 5\%$) with temperature or energy in the region 2–5 MK or 0.1–0.3 keV (Brown et al. 1998; Bhatia & Doschek 1992). The fact that most ratios observed in the Sun typically range from 1.5–2.8 (Brown et al. (1998), and references above), significantly lower than the theoretical ratios, supports claims that in solar active regions the 15.014 Å line is affected by resonant scattering. The 15.014/15.265 ratio which was recently measured in the Livermore Electron Beam Ion Trap (EBIT) (Brown et al. 1998) and ranges from 2.77–3.15 (with individual uncertainties of about $\pm$ 0.2) at energies between 0.85–1.3 keV, is significantly lower than calculated values. Although the EBIT results do not include probably minor contributions from processes such as dielectronic recombination satellites and resonant excitation, this may imply that the amount of solar scattering has been overestimated in past analyses. Our measured ratio Fe XVIII 16.078 Å/Fe XVII 15.265 Å

gives a temperature of $\sim$6 MK and the photon flux ratio 15.014/15.265 is measured to be 2.64$\pm$0.10. If we compare this to the recent EBIT results we conclude that there is little or no evidence for opacity effects in the 15.014 Å line seen in our Capella spectrum.

4. Conclusion

The Capella measurements with LETGS show a rich spectrum with excellent spectral resolution ($\Delta\lambda \simeq$0.06 Å, FWHM). About 150 lines have been identified of which the brightest hundred are presented in Table 1. The high-resolution spectra of the Chandra grating spectrometers allow us to carry out direct density diagnostics, using the He-like triplets of the most abundant elements in the LETGS-band, which were previously only possible for the Sun. Density estimates based on C, N and O He-like complexes indicate densities typical of solar active regions and some two or more orders of magnitude lower than density estimates for the hotter ($>$5 MK) plasma obtained from EUVE spectra. A preliminary investigation into the effect of resonance scattering in the Fe XVII line at 15.014 Å showed no clear evidence for opacity effects. After further LETGS in-flight calibration it is expected that relative Doppler velocities of the order of 30 km/s will be detectable at the longest wavelengths.

REFERENCES

Acton, L. W., Catura, R. C., Meyerott, A., & Wolfson, C. J. 1972, Solar Phys., 26, 183

Bhatia, A. K. & Doschek, G. A. 1992, At. Data Nucl. data Tables, 52, 1

Brickhouse, N. S., Raymond, J. C., & Smith, B. W. 1995, ApJS, 97, 551

Brinkman, A. C., et al. 1987, Astroph. lett. & comm., Vol. 26, 73–80

Brinkman, A. C., et al. 1997, SPIE, 3113, 181–192

Brown, G. V., Beiersdorfer, P., Liedahl, D. A., & Widmann, K. 1998, ApJ, 502, 1015

Catura, R. C., Acton, L. W., & Johnson, H. M. 1975, ApJ, 196, L47

Dupree, A. K., Brickhouse, N. S., Doschek, G. A., Green, J. C., & Raymond, J. C. 1993, ApJ, 418, L41

Gabriel, A. H. & Jordan, C. 1969, MNRAS, 145, 241–248

Hummel, C. A., Armstrong, J. T., Quirrenbach, A., Buscher, D. F., Mozurkewich, D., Elias, N. M. II, & Wilson, R. E. 1994, AJ, 107, 1859

Liedahl, D. A. 1999, private communication

Mason, H. E., Bhatia, A. K, Kastner, S. O., Neupert, W. M., & Swartz, M. 1984, Sol.Phys., 92, 199

Mewe, R. 1991, A&A Rev., 3, 127

Mewe, R., Gronenschild, E. H. B. M., & van den Oord, G. H. J. 1985, A&ASS, 62, 197

Mewe, R., Heise, J., Gronenschild, E. H. B. M., Brinkman, A. C., Schrijver, J., & den Boggende, A. J. F. 1975, ApJ, 202, L67

Mewe, R., Kaastra, J. S., & Liedahl, D. A. 1995, Legacy, 6, 16 (MEKAL)

Mewe, R., Lemen, J. R., & Schrijver, C. J. 1991, Ap&SS, 182, 35

Murray, S. S., et al. 1997, SPIE, 3114, 11

Phillips, K. J. H., Greer, C. J., Bhatia, A. K., Coffey, I. H., Barnsley, R., & Keenan, F. P. 1997, A&A, 324, 381

Phillips, K. J. H., Greer, C. J., Bhatia, A. K., & Keenan, F. P. 1996, ApJ, 469, L57

Phillips, K. J. H., Mewe, R., Harra-Murnion, L. K., Kaastra, J. S., Beiersdorf, P., Brown, G. V., & Liedahl, D. A. 1999, A&ASS, 138, 381

Pradhan, A. K. 1982, ApJ, 263, 477

Predehl, P., et al. 1997, SPIE, 3113, 172–180

Saba, J. L. R., Schmelz, J. T., Bhatia, A. K., & Strong, K. T. 1999, ApJ, 510, 1064

Schrijver, C. J., Mewe, R., van den Oord, G. H. J., & Kaastra, J. S. 1995, A&A, 302, 438

Van Speybroeck, L. P., Jerius, D., Edgar, R. J., Gaetz, T. J., & Zhao, P. 1997, SPIE, 3113, 89

Wolfson, C. J., Doyle, J. G., & Phillips, K. J. H. 1983, ApJ, 269, 319
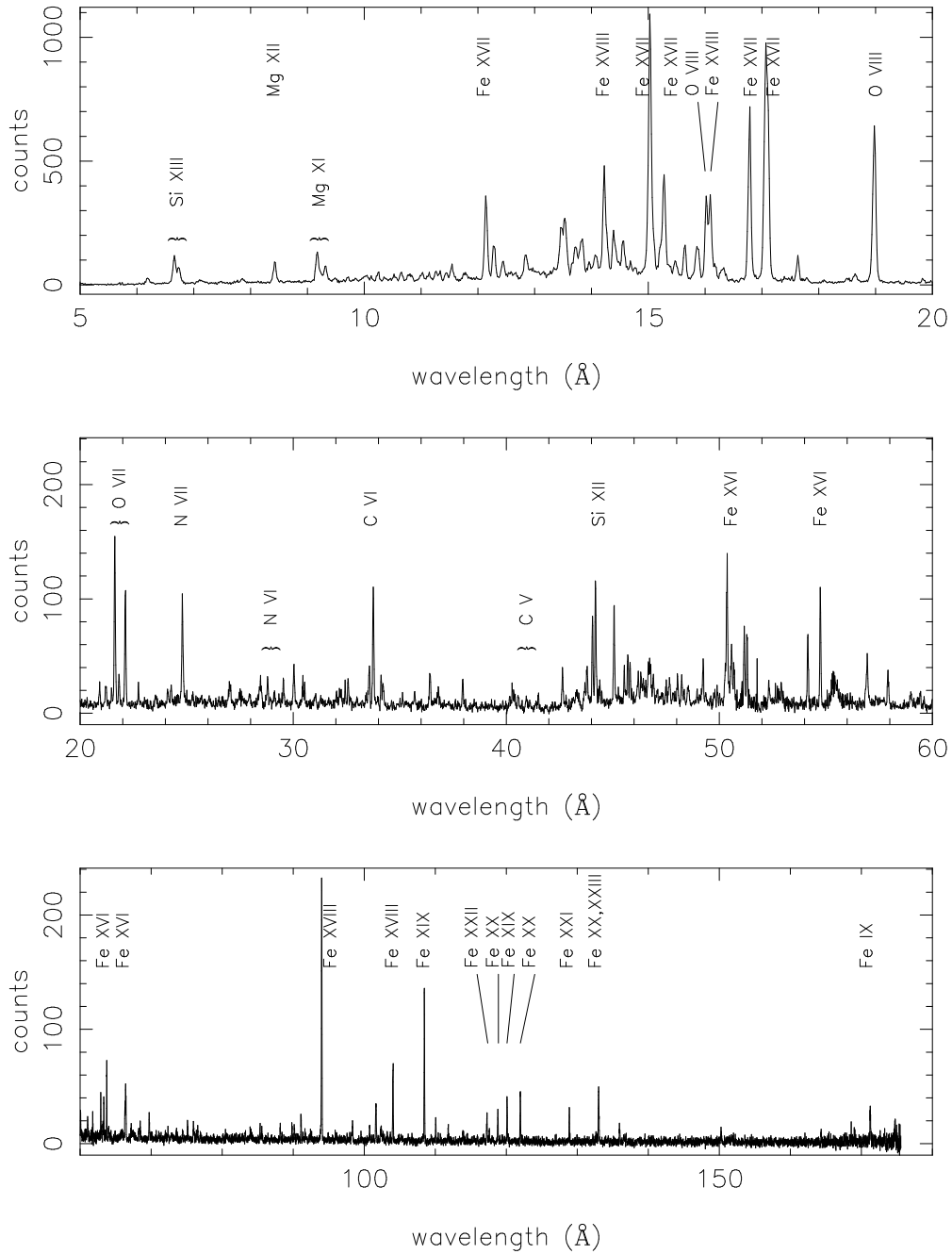
Fig. 1.— The complete LETGS spectrum of Capella, split into three parts for clarity. Note the difference in x and y scale for the three parts. Indicated in the plot are the triplets discussed in the text and a selection of the Fe lines at longer wavelengths. The hundred strongest lines are listed in Table 1.

Fig. 2.— The Oxygen VII triplet in the LETGS –1 order spectrum with the resonance (r), the forbidden (f), and the intercombination (i) line. The measured ratios of these lines (from the fitted curve) are given in the text.

Table 1.   Comparison of measured and theoretical values of the strongest lines in the Capella spectrum as shown in Fig. 1.

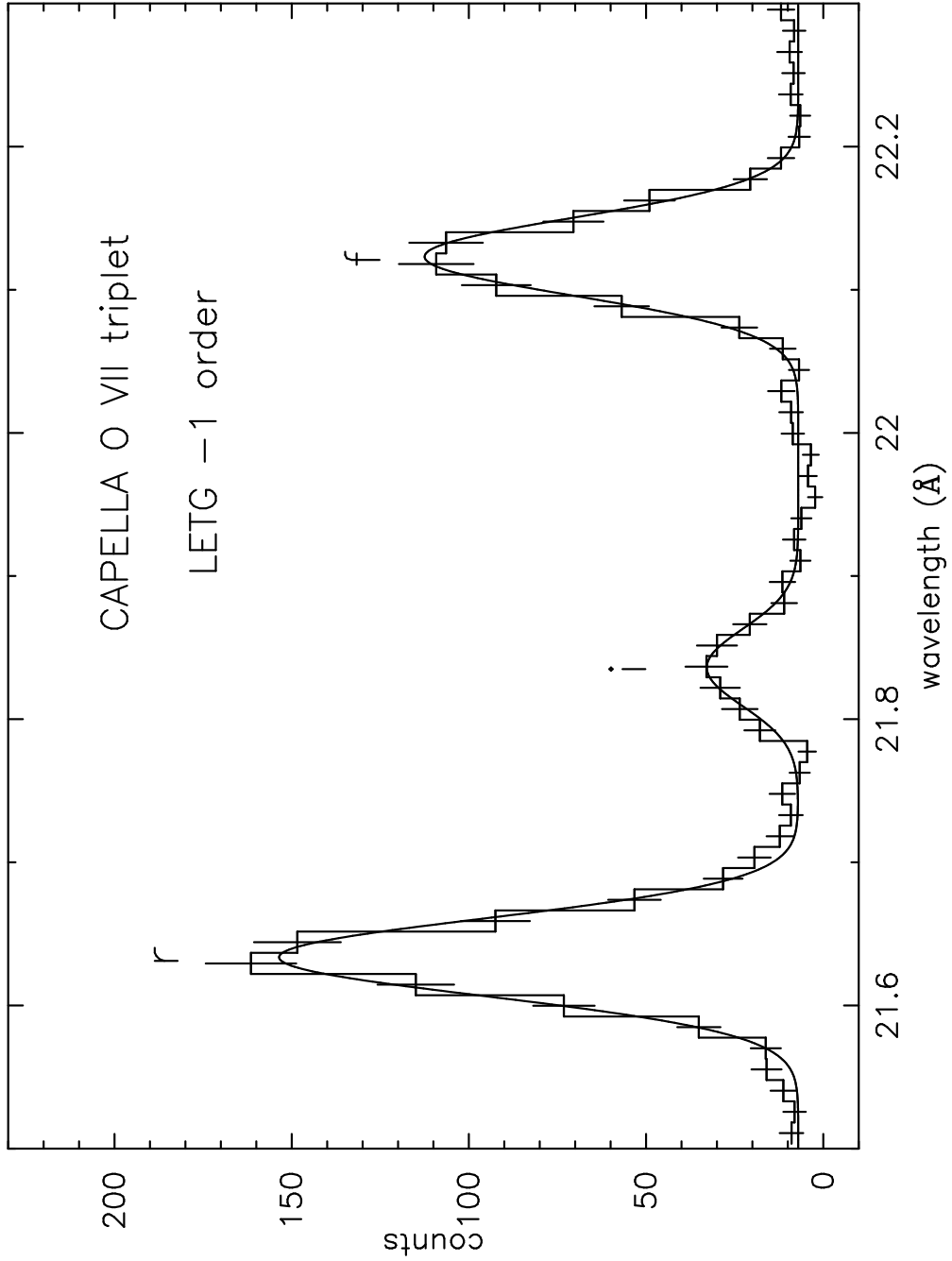| λ_{obs}	λ_{pred}	$\log(T_m)$	I	Ion		line ID
6.65	6.65	7.00	5.1	Si	XIII	He4w
6.74	6.74	7.00	2.9	Si	XIII	He6z
8.42	8.42	7.00	4.6	Mg	XII	H1AB
9.16	9.17	6.80	6.2	Mg	XI	He4w
9.31	9.32	6.80	3.1	Mg	XI	He6z
11.54b	11.55	6.60	3.5	Ne	IX	He3A
...	11.53	6.85		Fe	XVIII	F22
12.14b	12.13	6.80	16.8	Ne	X	H1AB
...	12.12	6.75		Fe	XVII	4C
12.27b	12.26	6.75	6.6	Fe	XVII	4D
...	12.29	7.00		Fe	XXI	C13
12.43	12.43	6.70	3.5	Ni	XIX	Ne5
12.84b	12.83	7.00	4.9	Fe	XX	N16
...	12.85	7.00		Fe	XX	N15
13.46	13.45	6.60	9.7	Ne	IX	He4w
13.53b	13.52	6.90	11.5	Fe	XIX	O1-68
...	13.51	6.90		Fe	XIX	O1-71
...	13.55	6.90		Ne	IX	He5xy
13.71	13.70	6.60	6.6	Ne	IX	He6z
13.82b	13.83	6.70	7.5	Fe	XVII	3A
...	13.84	6.90		Fe	XIX	O1-50
14.07	14.06	6.70	4.2	Ni	XIX	Ne8AB
14.22	14.21	6.80	18.0	Fe	XVIII	F1-56,55
14.27	14.26	6.80	5.3	Fe	XVIII	F1-52,53
14.38b	14.38	6.80	6.2	Fe	XVIII	F12
...	14.36	6.80		Fe	XVIII	F2-57,58
14.56b	14.54	6.80	5.3	Fe	XVIII	F10
...	14.56	6.80		Fe	XVIII	F9
15.02	15.01	6.70	44.2	Fe	XVII	3C
15.18b	15.18	6.60	3.4	O	VIII	H3
...	15.21	6.90		Fe	XIX	O4
15.27	15.27	6.70	16.7	Fe	XVII	3D
15.46	15.46	6.70	3.1	Fe	XVII	3E
15.64	15.63	6.80	6.2	Fe	XVIII	F7
15.83	15.83	6.80	4.3	Fe	XVIII	F6
15.88	15.87	6.80	4.4	Fe	XVIII	F5
16.02b	16.01	6.60	14.6	O	VIII	H2
...	16.00	6.80		Fe	XVIII	F4
16.08b	16.08	6.80	16.0	Fe	XVIII	F3
...	16.11	6.90		Fe	XIX	O2
16.30b	16.34	6.70	2.2	Fe	XVII	E2L
...	16.31	6.80		Fe	XVIII	F3-62

Table 1—Continued

λ_{obs}	λ_{pred}	$\log(T_m)$	I	Ion		line ID
16.78	16.78	6.70	27.9	Fe	XVII	3F
17.05	17.06	6.70	30.5	Fe	XVII	3G
17.10	17.10	6.70	29.5	Fe	XVII	M2
17.62	17.63	6.80	4.4	Fe	XVIII	F1
18.62b	18.63	6.80	2.0	Mg	XI	He6z(2)
...	18.63	6.30		O	VII	He3A
18.96	18.97	6.50	28.7	O	VIII	H1AB
21.61	21.60	6.30	6.5	O	VII	He4w(r)
21.82	21.80	6.30	1.1	O	VII	He5xy(i)
22.11	22.10	6.30	4.5	O	VII	He6z(f)
24.79	24.78	6.30	4.4	N	VII	H1AB
28.78	28.79	6.20	1.1	N	VI	He4w
29.52	29.53	6.20	0.9	N	VI	He6z
30.02	30.03	6.70	1.8	Fe	XVII	3C(2)
33.74	33.74	6.10	4.9	C	VI	H1AB
34.10	34.10	6.70	1.5	Fe	XVII	3G(2)
34.20	34.20	6.70	1.1	Fe	XVII	M2(2)
36.40b	36.37	6.70	1.4	Fe	XVII	4C(3)
...	36.40	6.30		S	XII	B6A
37.94	37.95	6.50	1.1	O	VIII	H1AB(2)
44.03b	44.02	6.30	3.3	Si	XII	Li6A
...	44.05	6.10		Mg	X	Li2
44.16	44.17	6.30	4.9	Si	XII	Li6B
45.03	45.04	6.70	4.2	Fe	XVII	3C(3)
45.68	45.68	6.30	1.9	Si	XII	Li7A
50.31	50.35	6.50	5.3	Fe	XVI	Na6A
50.55b	50.53	6.20	2.2	Si	X	B6A
...	50.56	6.50		Fe	XVI	Na6B
51.15	51.17	6.70	2.7	Fe	XVII	3G(3)
51.27	51.30	6.70	2.9	Fe	XVII	M2(3)
54.12	54.14	6.50	2.9	Fe	XVI	Na7B
54.71	54.73	6.50	4.4	Fe	XVI	Na7A
56.89	56.92	6.50	1.8	O	VIII	H1AB(3)
60.04	60.06	6.70	1.3	Fe	XVII	3C(4)
62.84	62.88	6.50	2.0	Fe	XVI	Na8B
63.68	63.72	6.50	2.9	Fe	XVI	Na8A
66.37	66.37	6.50	2.7	Fe	XVI	Na9A
68.20	68.22	6.70	1.0	Fe	XVII	3G(4)
68.40	68.40	6.70	1.2	Fe	XVII	M2(4)
75.06	75.07	6.70	0.8	Fe	XVII	3C(5)
75.87	75.89	6.50	0.9	O	VIII	H1AB(4)
85.24	85.28	6.70	0.8	Fe	XVII	3G(5)

Table 1—Continued

λ_{obs}	λ_{pred}	$\log(T_m)$	I	Ion	line ID
85.44	85.50	6.70	0.6	Fe XVII	M2(5)
90.08	90.08	6.70	1.0	Fe XVII	3C(6)
93.91	93.92	6.80	12.4	Fe XVIII	F4A
94.84	94.87	6.50	0.4	O VIII	H1AB(5)
101.55	101.55	6.90	2.5	Fe XIX	O6B
102.30	102.33	6.70	0.8	Fe XVII	3G(6)
102.57	102.60	6.70	0.4	Fe XVII	M2(6)
103.94	103.94	6.70	4.4	Fe XVIII	F4B
108.35	108.37	6.90	6.1	Fe XIX	O6A
113.79	113.84	6.50	0.5	O VIII	H1AB(6)
117.14	117.17	7.10	1.2	Fe XXII	B11
118.69	118.66	7.00	1.4	Fe XX	N6C
119.99	120.00	6.90	1.8	Fe XIX	O6D
121.86	121.83	7.00	2.0	Fe XX	N6B
128.74	128.74	7.00	1.6	Fe XXI	C6A
132.86b	132.85	7.00	4.0	Fe XX	N6A
...	132.85	7.10		Fe XXIII	Be13A
150.09	150.10	5.50	0.5	O VI	Li5AB
171.06	171.08	5.80	2.2	Fe IX	A4

Note. — $\lambda_{obs}, \lambda_{pred}$: observed and predicted line wavelengths (Å); T_m = temperature (in K) of maximum line formation; I = raw line intensity in 10^{-3} counts/sec. Note that these are included to illustrate approximate observed relative line strengths and do not represent definitive measurements.

b = blend with indication of a the most prominent lines in order of estimated decreasing strength.

ID = line identification; number in parentheses (m) indicates diffraction order $m > 1$.

For wavelengths and line identifications see Phillips et al. (1999) (solar and laboratory measurements between 5–20 Å), Mason et al. (1984) (solar observations between 90–175 Å), and Mewe, Gronenschild, & Van den Oord (1985); Mewe, Kaastra, & Liedahl (1995) (complete wavelength range in MEKAL).